

^2H NMR Theory of Transition Metal Dihydrides: Coherent and Incoherent Quantum Dynamics

Gerd Buntkowsky,^{*,†} Hans-Heinrich Limbach,[†] Frank Wehrmann,[†] Ingolf Sack,[†] Hans-Martin Vieth,[†] and Robert H. Morris[§]

Institut für Organische Chemie and Institut für Experimentalphysik der Freie Universität Berlin, Takustrasse 3, D-14195 Berlin, Germany, and Department of Chemistry, University of Toronto, 80 St. George Street, Toronto, Ontario, Canada M5S 3H6

Received: January 7, 1997; In Final Form: April 21, 1997[⊗]

In this paper a simple phenomenological description of the effects of coherent quantum and incoherent mutual exchange of two deuteron nuclei in solid state transition metal complexes on their ^2H NMR spectra is given. This description is based on the quantum-mechanical density matrix formalism developed by Alexander and Binsch. Only the nuclear spin system is treated quantum mechanically. The quantum exchange interaction in NMR is included in the nuclear spin Hamiltonian, and the interaction with the surrounding bath and incoherent exchange processes are treated as phenomenological rate processes described by rate constants. The incoherent exchange corresponds formally to 180° rotations or jumps of the D–D vector around an axis perpendicular to this vector and averages the different quadrupole splitting of the two deuterons. In principle the dideuteron pair will exist in several rovibrational states. However, if the interconversion among these states is fast, the dideuteron exchange can be described by an average exchange coupling or tunnel frequency X_{12} and a single average rate constant k_{12} of the incoherent exchange. It is shown that the incoherent exchange gives rise to a relaxation of rate $-2k_{12}$ between coherences created between states of different symmetry. The ^2H NMR line shape of a dideuteron pair in the solid state as a function of tunnel and incoherent exchange rate is studied numerically. For single crystals, the effects of coherent and incoherent exchange are strongly different, in particular if the rate constants are on the order of the quadrupole splitting. The spectra of nonoriented powder samples are more similar to each other. Nevertheless, our calculations show that there are still pronounced differences, which should allow the distinction between coherent and incoherent exchange even in nonoriented samples.

Introduction

The structure and dynamics of hydrogen in transition metal polyhydrides is a matter of current experimental and theoretical interest. Kubas et al.^{1,2} found dihydrogen units η -bound to the transition metal. Today, a whole series of transition metal polyhydrides with hydrogen distances varying between 0.8 and 1.7 Å is available.³ In these compounds the hydrogen atoms are mobile; in particular, they are subject to a mutual exchange, formally corresponding to 180° rotations involving a barrier with a height depending on the chemical structure. If the rotational barrier is zero, corresponding to free dihydrogen, the rotation is a coherent quantum process leading to even rotational states ($p\text{-H}_2$) with antiparallel nuclear spins and to odd rotational states ($o\text{-H}_2$) with parallel spins. When a rotational barrier is introduced by dihydrogen binding to a metal center, the energy splitting between the lowest $p\text{-H}_2$ and $o\text{-H}_2$ states corresponds to a coherent rotational tunnel splitting of frequency ν_t . This splitting can be observed by inelastic neutron scattering² (INS) when the barrier is small and the splittings are on the order of terahertz. In the other extreme, when the barrier is large and the tunnel splitting becomes of the order of typical ^1H chemical shift differences (i.e., hertz to kilohertz) the tunnel splitting gives rise to a quantum exchange coupling $X_{12} = J_{\text{exch}}$ in the NMR spectra^{4,5} of the hydride pairs, which can be observed if each hydride exhibits a different chemical shift. J_{exch} adds up with the usual scalar magnetic coupling J_{magn} to an effective J

coupling, as was recognized by Zilm et al.^{5a–d} and Weitekamp et al.^{5e} J_{exch} represents an average over a large number of rovibrational states as it increases strongly with increasing temperature. On the other hand, superimposed on the coherent exchange are incoherent exchange processes, which also have been observed in the NMR spectra of these hydrides^{4,6,7}. In the case of a HD pair, these incoherent processes correspond to H/D scrambling between the two different molecular sites in which the pair is located. In contrast to the quantum exchange, the incoherent exchange leads to a magnetic equivalence of the coupled hydrogen nuclei, i.e., to line broadening and coalescence. This process also leads to characteristic line shape changes in INS spectra² and affects the results of $p\text{-H}_2$ induced nuclear spin polarization experiments.⁸ These line shape changes can be described quantitatively in terms of the quantum-mechanical density matrix formalism developed by Alexander⁹ and Binsch,¹⁰ where only the nuclear spin degrees of freedom are treated quantummechanically and the spatial degrees of freedom (bath coordinates) are treated via phenomenological rate constants. The advantage of this formalism is that it is directly comparable to the NMR experiment, because NMR always measures the projection of the molecular system onto the spin system. Therefore it is possible to project the complex spatial dynamics of the problem onto these phenomenological rate constants that are measured in the NMR experiment. Thus a more detailed theory in the future only needs to reproduce these rate constants but not the NMR spectra from which these constants were extracted. We note that the phenomenological

* Corresponding author.

[†] Freie Universität Berlin.

[§] University of Toronto.

[⊗] Abstract published in *Advance ACS Abstracts*, June 1, 1997.

rate constants in the Alexander–Binsch formalism have recently been interpreted theoretically by Szymanski.¹¹

The dynamic range of NMR for the study of these tunnel processes is limited by the size of the typical frequency differences of the NMR method used. For the line shape analysis of ¹H NMR spectra this means that for a typical spectrometer a range of less than approximately 10 kHz is accessible in liquids. This range could, in principle, be extended by studying dipolar interactions in solid state ¹H NMR spectra, which are typically of the order of several tens of Kiloherz. However, in practice there exist several problems, which render this approach not very attractive: On the one hand, to avoid problems in the interpretation of the spectra caused by homogeneous broadening from bulk protons, one would prefer to study well-localized isolated proton pairs. On the other hand, however, since the spin wave functions of these proton pairs are symmetric under coherent or incoherent exchange (in the solid state, the chemical shift differences of protons are small compared to dipolar interactions to render the protons different), it would not be possible to detect the various exchange processes in the dipolar spectrum. Therefore, at least a third proton has to be employed, which renders the remaining two protons inequivalent and thus destroys the permutation symmetry.

Since, due to their low mass, only hydrogen isotopes exhibit this type of coherent tunnel couplings, the question arises whether pairs of deuterons can be used instead of protons to increase the dynamic range accessible by NMR spectroscopy. This will obviously not be the case for ²H liquid state NMR, because the typical spectral range is on the order of 1.5 kHz. However in the solid state, because deuterons are quadrupole nuclei, they exhibit electric quadrupolar interactions which are typically on the order of 100 kHz and for nonoriented samples give rise to the well-known line shape features in solid state ²H NMR spectra.^{12,13} ²H solid state NMR is particularly well suited for the investigation of exchanging deuterons, because the anisotropy of the quadrupole interaction typically found for these nuclei is a very sensitive probe for any type of nuclear motions inside the sample. Since the quadrupole interaction reflects the symmetry of the electric field gradient tensor at the position of the nucleus studied, it is a very efficient measure of its electronic binding characteristics.

In this paper, we explore the possibility of extracting exchange couplings (coherent rotational tunnel splittings) as well as rate constants of the incoherent exchange of suitably labeled transition metal polyhydrides from solid state ²H NMR in the regime up to 100 kHz using the Alexander–Binsch theory. We note that this theory has been applied recently in order to describe the ²H NMR spectra of deuterated methyl groups^{14d} in ordered samples (single crystals) in the presence of coherent and incoherent rotations. As single crystals suitable for ²H NMR are not easily available in the case of transition metal polyhydrides, we are especially concerned in calculating spectra of non-oriented samples (crystalline powders). We are mainly concerned with the discrimination between coherent tunneling and incoherent exchange processes, both of which can be present in the sample under investigation. While in general this can easily be achieved for the ²H NMR spectra of single crystals or liquid samples, this can be a very difficult task in the case of nonoriented samples, because of the distribution of resonance frequencies in these spectra.

The rest of this paper is organized as follows: After a brief discussion of the relevant terms in the Hamiltonian of two coupled deuterons, a short summary of the generalized Alexander–Binsch formalism including a general form of the incoherent self-exchange operator is given. Next follows a short description of the numerical methods used for calculating the

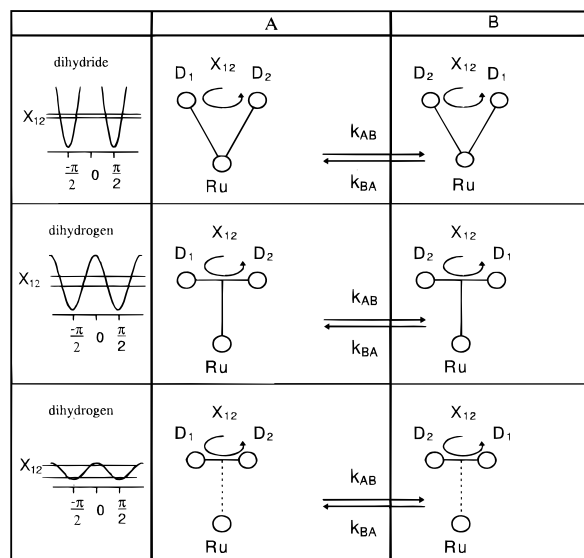


Figure 1. Scheme of coherent and incoherent exchange processes in a Me–D₂ system for various configurations. Left column: symbolic shape of potential. Middle column: configuration A, deuteron 1 is on the left side, and deuteron 2 is on the right side, corresponding to subspace A of the composite Liouville space. Right column: configuration B, deuteron 2 is on the left side, and deuteron 1 is on the right side, corresponding to subspace B of the composite Liouville space. Top row: dihydride, deuterons are tightly bound to the metal, deep potential depth and small tunnel splitting. Middle row: dihydrogen, deuterons form bonds of medium strength to the metal and to each other, intermediate potential depth and tunnel splitting. Bottom row: dihydrogen, deuterons are only weakly bound to the metal and tightly bound to each other, shallow potential and large tunnel splitting. X₁₂ is the coherent tunnel splitting, which can be visualized as a rotation of the deuterons with frequency X₁₂ between the two potential minima in each configuration, taking place only in one subspace of the composite Liouville space. k_{AB}, k_{BA} are the rates of incoherent exchange of the deuterons between configurations A and B, which connect the different subspaces of the composite Liouville space.

TABLE 1: Hilbert Space Base Functions

$ b_1\rangle = ++\rangle$	$ b_2\rangle = +0\rangle$	$ b_3\rangle = +-\rangle$
$ b_4\rangle = 0+\rangle$	$ b_5\rangle = 00\rangle$	$ b_6\rangle = 0-\rangle$
$ b_7\rangle = -+\rangle$	$ b_8\rangle = -0\rangle$	$ b_9\rangle = --\rangle$

spectra, and then some typical numerical results are shown and discussed. For the convenience of the reader we have included in Tables 1, 2, and 3 Hilbert space base functions, matrix representations, eigenvalues, and eigenvectors of the combined quadrupolar and quantum exchange Hamiltonian of a D₂-system.

Theory

A system of two hydrogen atoms (either ¹H or ²H) bound to a transition metal is studied. The dihydrogen rotation then involves a barrier but remains a quantum process similar to the case of free dihydrogen, involving delocalized rotational *p*-H₂ and *o*-H₂ state pairs. The quantum rotation can be characterized by a rotational tunnel frequency corresponding at low temperatures to the energy splitting of the lowest rotational state pair. There are two limiting cases: Either the two hydrogen atoms form a dihydrogen state, which is only loosely bound to the metal and behaves more or less like a free hydrogen molecule, or in the other extreme, each hydrogen is directly bound to the metal, leading to a dihydride.

A schematical picture of these exchange processes is depicted in Figure 1. For the ¹H case, unusually large *J*-couplings were observed in these compounds, which have been identified as exchange couplings by Weitekamp and Zilm,⁵ arising from the fact that the spatial symmetry of the wave functions imposes restrictions on the allowed combinations of spin and spatial wave

TABLE 2: Matrix Representation of Tunnel and Quadrupole Hamiltonian^a

$$\hat{H} = \begin{pmatrix} X_{12} + \frac{2}{3}Q & 0 & 0 & 0 & 0 & 0 & 0 & 0 & 0 \\ 0 & -\frac{1}{3}Q - q & 0 & X_{12} & 0 & 0 & 0 & 0 & 0 \\ 0 & 0 & \frac{2}{3}Q & 0 & 0 & 0 & X_{12} & 0 & 0 \\ 0 & X_{12} & 0 & -\frac{1}{3}Q + q & 0 & 0 & 0 & 0 & 0 \\ 0 & 0 & 0 & 0 & X_{12} - \frac{4}{3}Q & 0 & 0 & 0 & 0 \\ 0 & 0 & 0 & 0 & 0 & -\frac{1}{3}Q + q & 0 & X_{12} & 0 \\ 0 & 0 & X_{12} & 0 & 0 & 0 & \frac{2}{3}Q & 0 & 0 \\ 0 & 0 & 0 & 0 & 0 & X_{12} & 0 & -\frac{1}{3}Q - q & 0 \\ 0 & 0 & 0 & 0 & 0 & 0 & 0 & 0 & X_{12} + \frac{2}{3}Q \end{pmatrix}$$

$$^a Q = (1/2)(q_1 + q_2); q = (1/2)(q_1 - q_2).$$

TABLE 3: Eigenvalues and Eigenfunctions of the Combined Tunnel and Quadrupole Hamiltonian. They Split into Two Singlets, Two Doublets and One Triplet

$E_{1,2,3} = \frac{2}{3}Q + X_{12}$	$ ++\rangle, --\rangle, \frac{ +-\rangle + -+\rangle}{\sqrt{2}}$
$E_{4,5} = -\frac{1}{3}Q - \sqrt{X_{12}^2 + q^2}$	$\frac{\cos(\varphi) -0\rangle - \sin(\varphi) 0-\rangle}{\sqrt{2}}, \frac{-\sin(\varphi) 0+\rangle + \cos(\varphi) +0\rangle}{\sqrt{2}}$
$E_{6,7} = -\frac{1}{3}Q + \sqrt{X_{12}^2 + q^2}$	$\frac{\cos(\varphi) 0-\rangle + \sin(\varphi) -0\rangle}{\sqrt{2}}, \frac{\sin(\varphi) +0\rangle + \cos(\varphi) 0+\rangle}{\sqrt{2}}$
$E_8 = -\frac{4}{3}Q + X_{12}$	$ 00\rangle$
$E_9 = \frac{2}{3}Q - X_{12}$	$\frac{- +-\rangle + -+\rangle}{\sqrt{2}}$

$$\tan(\varphi) = \frac{q + \sqrt{X_{12}^2 + q^2}}{X_{12}}$$

functions (antisymmetrizing postulate). As was already realized by Dirac,¹⁵ for a system of two coupled spin- $1/2$ particles, the spin alone is able to characterize the four lowest eigenstates of the system, and therefore he introduced a spin exchange operator V_{exch} acting on the spin functions alone. Except for the trivial absolute shift of the energies by $J_{\text{exch}}/4$, the spin exchange operator acts as the usual spin-spin coupling Hamiltonian used in NMR. Thus, both Hamiltonians are indistinguishable, and in NMR their sum will always be observed. Therefore, the exchange coupling J_{exch} can be combined with the normal magnetic spin coupling constant J_{magn} to an effective coupling constant J giving the total energy between the nuclear triplet and singlet spin states of a pair of two hydrogen nuclei, i.e.

$$J = J_{\text{magn}} + J_{\text{exch}} \quad (1)$$

For deuterons, however, the spin-spin coupling Hamiltonian and the tunnel Hamiltonian are no longer equivalent and can be distinguished due to their different energy spectrum, and thus the tunnel splitting can be directly measured by NMR, as has been shown in several ^2H NMR studies of deuterated methyl group tunneling by solid state NMR¹⁴. Note: to account for this difference, in the following the exchange coupling of the two deuterons is labeled as X_{12} .

In parallel to this coherent exchange or tunneling of the two deuterons, there can exist a second kind of process, the incoherent exchange of the two deuterons. Characteristic for coherent tunneling is that the Hamiltonian of the spin system does not depend explicitly on the time during the evolution of the spin dynamics, i.e. all interactions with external bath degrees of freedom are negligible. However, for example due to molecular motions, vibrations, or reorientations, the Hamiltonian itself can change in the course of the NMR experiment, which

will give rise to some form of relaxation as long as the correlation times of the motion are on the order of the energy differences in the Hamiltonian. The phenomenon of incoherent exchange of two protons or deuterons or of a proton and a deuteron between different atomic sites of polyatomic molecules has been observed in various compounds, for example in porphyrins and chlorins, where the incoherent exchange dynamics has been followed by liquid and solid state NMR.^{16a-c}

Moreover, there exists another type of motion, which has been investigated recently^{16d} and which can be depicted as follows. The energetically highly excited states of the molecule exhibit only small thermal populations, due to their Boltzmann factors. In general, these states exhibit a much larger tunnel splitting than do the more populated states of lower energy, which will result in a fast-evolving spin dynamics. If the lifetime of these states is sufficiently short, they will not contribute to the average tunnel frequency. However, the fast spin dynamics will lead to an apparently incoherent exchange of the two hydrogens with an exchange rate which is mainly determined by the population rate of this state. We wish to remark that in systems of four or more coupled spins it is possible to distinguish this type of apparently incoherent process from the previous ones.

Hamiltonians and Coherent Dynamics. The NMR Hamiltonian of a system of two deuterons in the solid state can be written in the following form:

$$\hat{H} = \hat{H}_{\text{CS}} + \hat{H}_X + \hat{H}_Q + \hat{H}_J + \hat{H}_D \quad (2)$$

In this equation, \hat{H}_{CS} is the shielding Hamiltonian, \hat{H}_X is the tunneling Hamiltonian, \hat{H}_Q is the quadrupole Hamiltonian, \hat{H}_D

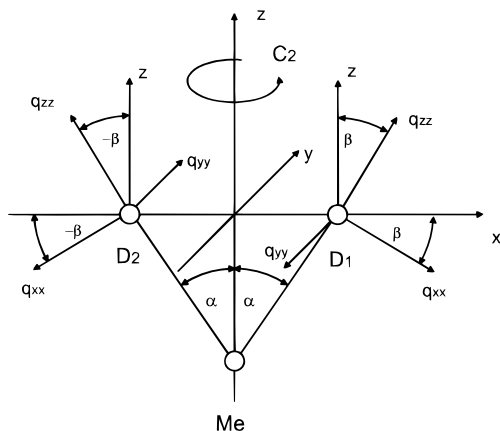


Figure 2. Coordinate system used for describing the relative spatial orientation of the two quadrupole tensors of deuterons D_1 and D_2 . C_{2v} symmetry is assumed for the deuterons, and therefore one of the principal axes (q_{yy}) is parallel to y . The quadrupole tensor of deuteron 2 is obtained by a 180° rotation around the z -axis of the coordinate system. For describing the relative orientations of the tensors it is more convenient to use the angle between the z -axis and the q_{zz} -component. Note that in general $\alpha \neq \beta$.

is the dipolar coupling Hamiltonian, and \hat{H}_J is the spin–spin coupling Hamiltonian. The five Hamiltonians in the presence of a strong magnetic field can be written as:

$$\hat{H}_Q = q_1(3\hat{I}_{z1}^2 - 2) + q_2(3\hat{I}_{z2}^2 - 2) \quad (3)$$

$$\hat{H}_{CS} = \nu_1 \hat{I}_{z1} + \nu_2 \hat{I}_{z2}$$

$$\hat{H}_X = X_{12} \hat{P}(\hat{\mathbf{I}}_1, \hat{\mathbf{I}}_2)$$

$$\hat{H}_D = D_{12}(3\hat{I}_{z1}\hat{I}_{z2} - \hat{\mathbf{I}}_1\hat{\mathbf{I}}_2)$$

$$\hat{H}_J = J_{12}\hat{\mathbf{I}}_1\hat{\mathbf{I}}_2$$

In these equations, ν_1 and ν_2 are the chemical shift values of the two spins, X_{12} is the coherent tunnel frequency, $\hat{P}(\hat{\mathbf{I}}_1, \hat{\mathbf{I}}_2)$ is the permutation operator¹⁷ of the two spins $\hat{\mathbf{I}}_1$ and $\hat{\mathbf{I}}_2$, D_{12} is the dipolar coupling among the spins, q_1 and q_2 are the quadrupole couplings of the spins, and J_{12} is the value of the spin–spin coupling. While for protons, the spin–spin coupling Hamiltonian and the tunneling Hamiltonian are of the same form, giving rise to an effective J -coupling as mentioned above, this is not the case for $I > 1/2$. In general, the various frequencies appearing in the Hamiltonians of eqs 2 and 3 can be time dependent, for example due to molecular motions or chemical reactions.

In a first approximation in the solid state, we can restrict ourselves to consider only the leading interactions, i.e. the quadrupole interaction and the coherent tunnel exchange:

$$\hat{H} = \hat{H}_{CS} + \hat{H}_X \quad (4)$$

In contrast to the coherent exchange interaction, the quadrupole interaction depends on the relative orientation of the magnetic field to the quadrupole tensor. Since both deuterons can be assumed to be chemically equivalent, their quadrupole tensors are related by a geometrical transformation. If we assume C_{2v} symmetry of the Me– D_2 group by neglecting possible crystal effects, one of the three principal axes of the quadrupole tensor will be perpendicular to the Me– D_2 plane, and the axis bisecting the bond angle (2α) will be a 2-fold symmetry axis (C_2). A coordinate system (see Figure 2) is chosen in such a way that the z -axis bisects the bond angle and that the y -axis is perpendicular to the bond plane. The two quadrupole tensors are related by a rotation \mathbf{R} with angles $\pm\beta$

around the y -axis of the coordinate system, i.e. in the given coordinate system the following equations for the quadrupole tensors $\vec{\mathbf{Q}}_1$ and $\vec{\mathbf{Q}}_2$ are obtained ($\vec{\mathbf{Q}}_{PAS}$: quadrupole tensor in its principal axis system)

$$\vec{\mathbf{Q}}_1 = \mathbf{R} \vec{\mathbf{Q}}_{PAS} \mathbf{R}^{-1} \quad (5)$$

$$\vec{\mathbf{Q}}_2 = \mathbf{R}^{-1} \vec{\mathbf{Q}}_{PAS} \mathbf{R}$$

with the rotation matrix \mathbf{R} given as

$$\mathbf{R} = \begin{pmatrix} \cos(\beta) & 0 & -\sin(\beta) \\ 0 & 1 & 0 \\ \sin(\beta) & 0 & \cos(\beta) \end{pmatrix} \quad (6)$$

The angle β depends on the strength of the electric field gradients caused by the metal and by the other deuterons. In particular in the case of a dihydride, β will be half the bond angle (i.e. $\beta = \alpha$), while for a pure dihydrogen complex, $\beta = \pi/2$. From this we get for $\vec{\mathbf{Q}}_1$ and $\vec{\mathbf{Q}}_2$ (q_{xx} , q_{yy} , and q_{zz} are the principal values of the quadrupole interaction):

$$\vec{\mathbf{Q}}_{1,2} = \begin{pmatrix} q_{xx} \cos^2(\beta) + q_{zz} \sin^2(\beta) & 0 & \pm(q_{xx} - q_{zz}) \cos(\beta) \sin(\beta) \\ 0 & q_{yy} & 0 \\ \pm(q_{xx} - q_{zz}) \cos(\beta) \sin(\beta) & 0 & q_{xx} \cos^2(\beta) + q_{zz} \sin^2(\beta) \end{pmatrix} \quad (7)$$

If \mathbf{b} is a unit vector pointing into the direction of the magnetic field

$$\mathbf{b} = \mathbf{B}_0/B_0 = (\sin(\vartheta) \cos(\varphi), \sin(\vartheta) \sin(\varphi), \cos(\vartheta)) \quad (8)$$

the quadrupole transition frequencies as a function of the polar angles can be calculated by the scalar product:

$$q_{1,2}(\vartheta, \varphi) = \mathbf{b} \vec{\mathbf{Q}}_{1,2} \mathbf{b} \quad (9)$$

The coherent tunnel exchange can be described by the permutation operator $\hat{P}(\hat{\mathbf{I}}_1, \hat{\mathbf{I}}_2)$ times the tunnel frequency X_{12} , i.e.:

$$\hat{H}_X = X_{12} \hat{P}(\hat{\mathbf{I}}_1, \hat{\mathbf{I}}_2) \quad (10)$$

In the product base of the two spins, the matrix representation of $\hat{P}(\hat{\mathbf{I}}_1, \hat{\mathbf{I}}_2)$ can be easily calculated from

$$\hat{P}(\hat{\mathbf{I}}_1, \hat{\mathbf{I}}_2)|\mu\nu\rangle = |\nu\mu\rangle \quad (11)$$

In the absence of incoherent exchange processes, the whole dynamics of the system can be described directly in the Hilbert space of \hat{H} , and thus the spectra can be calculated directly from \hat{H} . However, as soon as incoherent exchange mechanisms are present, this approach is no longer valid. A method for tackling this type of problems is the Alexander–Binsch formalism described in the next section.

Generalized Alexander–Binsch Theory and Incoherent Dynamics. In this section a formulation of coherent and incoherent exchange processes of dihydrogen and dideuterium is given, using a framework which is a generalized version of the original Alexander–Binsch theory for the calculation of exchange broadened NMR spectra. The idea behind this theory is to represent a fluctuating time dependence of the parameters in the Hamiltonian of eq 3 as an exchange between several molecular configurations (denoted by capital letters A, B, ...)

with an exchange rate which is determined by the rate of the fluctuation. In the following, for brevity these molecular configurations are called states.

The model of an asymmetric intermolecular exchange between different dihydrogen states is considered, for example a bound state and a free state or two different bound states. For this system the effects of intramolecular self-exchange (i.e. permutation of the two hydrogen atoms) in the various states on the density matrix and the resulting spectra are calculated.

The various dihydrogen states (n) are characterized by their basic spin Hamiltonians \hat{H}_n . From these state Hamiltonians the state Liouville superoperators are constructed following the procedure given by Ernst et al.¹⁸ (\hat{E}_n is the unit matrix of Hilbert space n , \hat{H} is the transpose of \hat{H}):

$$\hat{L}_n = \hat{H}_n \otimes \hat{E}_n - \hat{E}_n \otimes \hat{H}_n, \quad n = A, B, \dots \quad (12)$$

The different states are described as vectors $|\rho_n\rangle$ in a composite Liouville space which correspond to the standard density matrix in Hilbert space. The dynamics of these vectors is governed by linear superoperators \hat{W}_n . It is assumed that all exchange processes are first-order reactions which can be described by simple rate constants k_{mn} . In the following, only two states are considered ($n = 1, 2$) and the equations of motion of the density matrices in the two states are

$$\frac{d}{dt}|\rho_1\rangle = -\hat{W}_1|\rho_1\rangle - k_{12}|\rho_1\rangle + k_{21}|\rho_2\rangle \quad (13)$$

$$\frac{d}{dt}|\rho_2\rangle = -\hat{W}_2|\rho_2\rangle - k_{21}|\rho_2\rangle + k_{12}|\rho_1\rangle$$

The superoperator $\hat{W}_n = \hat{R}_n + i\hat{L}_n$ describes the dynamics in one state. It consists of a coherent term \hat{L}_n , the Liouville superoperator of state n , stemming from the Hamiltonian \hat{H}_n , and an incoherent term, \hat{R}_n , the relaxation superoperator in state n . The equation for the density matrix can be formulated as a matrix equation in composite Liouville space, introducing the overall density matrix $|\rho\rangle$, which is the direct sum over all sites.

$$|\rho\rangle = |\rho_1\rangle \oplus |\rho_2\rangle \quad (14)$$

$$\hat{W} = \hat{W}_1 \oplus \hat{W}_2 \quad (15)$$

The different states are connected by the exchange superoperator \hat{K} , which can be constructed by forming the direct product of the exchange matrix that describes the kinetics with the identity matrix \hat{I}_d of one of the individual subspaces of the composite Liouville space:

$$\hat{K} = \begin{pmatrix} -k_{12} & k_{21} \\ k_{12} & -k_{21} \end{pmatrix} \otimes \hat{I}_d \quad (16)$$

This gives the following equation for the overall density matrix:

$$\frac{d}{dt}|\rho\rangle = -\hat{W}|\rho\rangle - \hat{K}|\rho\rangle \quad (17)$$

If the system is treated at finite temperature, the equilibrium density matrix $|\rho\rangle$ will be different from zero, and eventually the Liouville–von Neumann equation is obtained as the kinetic equation of the density matrix

$$\frac{d}{dt}|\rho\rangle = -(\hat{W} + \hat{K})|\rho\rangle =: -\hat{M}|\rho\rangle \quad (18)$$

where \hat{M} has been introduced as the dynamic superoperator. The formal solution of this equation is

$$|\rho(t)\rangle = \exp(-\hat{M}t)|\rho(0) - \rho_\infty\rangle + |\rho_\infty\rangle \quad (19)$$

The Incoherent Self-Exchange Superoperator for a Double Hydrogen Transfer. A particularly simple exchange problem is the incoherent mutual exchange of two equal nuclei, for example the mutual exchange of two protons or two deuterons, corresponding to a permutation of the two nuclei which exchanges the chemical shift values and quadrupole couplings in eq 3. In this case, because of the symmetry of the problem, it follows that $k_{12} = k_{21} = k$.

The Hamiltonian of the system consists of three parts: the individual Hamiltonians of the spins \hat{I}_1, \hat{I}_2 , which are most easily described by assigning them to molecular sites $m = 1, 2$, i.e.; $\hat{H}_m(\hat{I}_m)$, Hamiltonian of spin n in site m ; a Hamiltonian $\hat{H}_{12}(\hat{I}_1, \hat{I}_2)$ representing the coupling between the spins. The incoherent process is then a permutation of the individual Hamiltonians with rate k , i.e.:

$$\begin{array}{ccc} \hat{H}_1(\hat{I}_1) & & \hat{H}_2(\hat{I}_1) \\ & \xleftrightarrow{k} & \\ \hat{H}_2(\hat{I}_2) & & \hat{H}_1(\hat{I}_2) \end{array} \quad (20)$$

The coupling Hamiltonian, which is symmetric in the two spins, is not affected by the permutation, i.e.: $[\hat{P}(\hat{I}_1, \hat{I}_2), \hat{H}_{12}(\hat{I}_1, \hat{I}_2)] = 0$. Thus the incoherent process can be regarded as a fluctuation between \hat{H}_A and \hat{H}_B with the rate k :

$$\hat{H}_A = \hat{H}_1(\hat{I}_1) + \hat{H}_2(\hat{I}_2) + \hat{H}_{12}(\hat{I}_1, \hat{I}_2) \quad (21)$$

$$\hat{H}_B = \hat{H}_2(\hat{I}_1) + \hat{H}_1(\hat{I}_2) + \hat{H}_{12}(\hat{I}_2, \hat{I}_1)$$

The equations of motion for the density operator (eq 13) reduce to

$$\frac{d}{dt}|\rho_A\rangle = -\hat{W}_A|\rho_A\rangle - k|\rho_A - \rho_B\rangle \quad (22)$$

$$\frac{d}{dt}|\rho_B\rangle = -\hat{W}_B|\rho_B\rangle - k|\rho_B - \rho_A\rangle$$

In Liouville space, the permutation of the two nuclei is described by a permutation superoperator \hat{P}_{12} , which is constructed from the permutation operator in Hilbert space $\hat{P}(\hat{I}_1, \hat{I}_2)$, using the rule for unitary transformation superoperators given in ref 18 ($\hat{P}(\hat{I}_1, \hat{I}_2)^*$, complex conjugate of $\hat{P}(\hat{I}_1, \hat{I}_2)$):

$$\hat{P}_{12} = \hat{P}(\hat{I}_1, \hat{I}_2) \otimes \hat{P}(\hat{I}_1, \hat{I}_2)^* \quad (23)$$

Since \hat{P}_{12} is a permutation superoperator, applying it twice gives the identity

$$\hat{P}_{12}\hat{P}_{12} = \hat{I}_d \quad (24)$$

The permutation symmetry of the nuclei is then expressed as

$$\hat{W}_A = \hat{P}_{12}\hat{W}_B\hat{P}_{12}^{-1} \quad (25)$$

In a matrix representation the equation of motion for the density matrix in composite Liouville space has the following form.

$$\frac{d}{dt} \begin{pmatrix} \rho_A \\ \rho_B \end{pmatrix} = \begin{pmatrix} -\hat{W}_A - k\hat{I}_d & kI_d \\ kI_d & -\hat{W}_B - k\hat{I}_d \end{pmatrix} \begin{pmatrix} \rho_A \\ \rho_B \end{pmatrix} \quad (26)$$

This equation can be transformed by applying the superoperator

$$\begin{pmatrix} \hat{I}_d & 0 \\ 0 & \hat{P}_{12} \end{pmatrix} \quad (27)$$

into

$$\frac{d}{dt} \begin{pmatrix} \rho_A \\ \hat{P}_{12}\rho_B \end{pmatrix} = \begin{pmatrix} -\hat{W}_A - k\hat{I}_d & k\hat{P}_{12} \\ k\hat{P}_{12} & -\hat{W}_A - k\hat{I}_d \end{pmatrix} \begin{pmatrix} \rho_A \\ \hat{P}_{12}\rho_B \end{pmatrix} \quad (28)$$

In a second step, the symmetric ρ_g (gerade) and antisymmetric ρ_u (ungerade) linear combinations of ρ_A and $\hat{P}_{12}\rho_B$ are formed and the differential equations are decoupled:

$$\frac{d}{dt} \begin{pmatrix} \rho_g \\ \rho_u \end{pmatrix} = \frac{d}{dt} \begin{pmatrix} \rho_A + \hat{P}_{12}\rho_B \\ \rho_A - \hat{P}_{12}\rho_B \end{pmatrix} = \begin{pmatrix} -\hat{W}_A - k\hat{I}_d + k\hat{P}_{12} & 0 \\ 0 & -\hat{W}_A - k\hat{I}_d - k\hat{P}_{12} \end{pmatrix} \begin{pmatrix} \rho_g \\ \rho_u \end{pmatrix} \quad (29)$$

Thus a projection of the complete Liouville space onto the symmetric L_g and antisymmetric L_u subspace is applied. Because of the symmetry of the states, the initial condition in normal NMR experiments will be $|\rho_A(0)\rangle = \hat{P}_{12}|\rho_B(0)\rangle$ and thus the antisymmetric density matrix is zero, $\rho_u = 0$ initially and hence for all times, and only the symmetric subspace L_g has to be considered in the time evolution of the density matrix, which gives the following equation for ρ_g

$$\frac{d}{dt} |\rho_g\rangle = (-\hat{W}_A - k\hat{I}_d + k\hat{P}_{12}) |\rho_g\rangle = -(\hat{W}_A + \hat{K}) |\rho_g\rangle \quad (30)$$

where the self-exchange superoperator \hat{K} has been introduced as

$$\hat{K} = -k(\hat{I}_d - \hat{P}_{12}) \quad (31)$$

This formal derivation of the self-exchange can be interpreted in a physical picture. In the symmetric linear combination of the individual density matrices, the two spins have lost their individuality. However, the individual Hamiltonians are still distinct and correspond usually to different molecular or, more generally, different spatial sites. Thus, the labeling of the spins is done via these sites (1,2); hence, it is called site labeling.

To understand the physical properties of the self exchange operator, it is most useful to represent the permutation operator $\hat{P}(\hat{\mathbf{I}}_1, \hat{\mathbf{I}}_2)$ in the permutation symmetry-adapted base of the Hilbert space (noted by $\hat{\cdot}$). The permutation operator in this base, $\hat{P}'(\hat{\mathbf{I}}_1, \hat{\mathbf{I}}_2)$, is diagonal, with matrix elements +1 for even (gerade) and -1 for odd (ungerade) states.¹⁷

$$\hat{P}'(\hat{\mathbf{I}}_1, \hat{\mathbf{I}}_2) := (-1)^\mu \delta_{ij}, \quad \mu = 0 \text{ if state } |i\rangle \text{ is gerade, } 1 \text{ if ungerade} \quad (32)$$

The matrix elements of the permutation superoperator in Liouville space, \hat{P}'_{12} , are (for simplicity double indices from

the Hilbert space base are used for the Liouville space)

$$\begin{aligned} (\hat{P}'_{12})_{ij,kl} &= (\hat{P}'(\hat{\mathbf{I}}_1, \hat{\mathbf{I}}_2) \otimes \hat{P}'(\hat{\mathbf{I}}_1, \hat{\mathbf{I}}_2)^*)_{ij,kl} \quad (33) \\ &= (-1)^\mu \delta_{ij} (-1)^\nu \delta_{kl} \\ &= (-1)^{\mu+\nu} \delta_{ij} \delta_{kl} \\ &= \begin{cases} +1 & \mu = \nu \\ -1 & \mu \neq \nu \end{cases} \end{aligned}$$

From this it follows for the diagonal elements of \hat{P}'_{12} that they are either +1 if states of the same symmetry are connected ($\mu = \nu$) or -1 if states of different symmetry are connected ($\mu \neq \nu$). The matrix elements of the self-exchange superoperator, eq 31, are given as

$$\begin{aligned} (\hat{K}')_{ij,kl} &= (-k(\hat{I}'_d - \hat{P}'_{12}))_{ij,kl} \quad (34) \\ &= -k(\delta_{ij} \delta_{kl} - (-1)^{\mu+\nu} \delta_{ij} \delta_{kl}) \\ &= -k \delta_{ij} \delta_{kl} (1 - (-1)^{\mu+\nu}) \\ &= \begin{cases} 0 & \mu = \nu \\ -2k & \mu \neq \nu \end{cases} \end{aligned}$$

Thus in this base, the self-exchange superoperator is also diagonal, with matrix elements 0 if states of the same symmetry are connected and matrix elements $-2k$ if states of different symmetry are connected. This result can be interpreted in a simple physical picture: In the symmetry-adapted base, the self-exchange operator acts as a relaxation operator for coherences created between the states of different symmetry, which relax with the rate $-2k$.

The essence of the Alexander-Binsch formalism described above is that the whole kinetics of the Me-D₂ system can be described by two empirical constants, the incoherent exchange constant k_{12} and the coherent tunnel exchange constant X_{12} . In general these two constants represent the thermal average of the tunnel splitting and the exchange constants, respectively, of the populated levels and thus will exhibit a nontrivial temperature dependence ($p_\xi(T)$ is the thermal population of level ξ):

$$k_{12}(T) = \sum_{\xi} p_\xi(T) k_{12\xi} \quad (35)$$

$$X_{12}(T) = \sum_{\xi} p_\xi(T) X_{12\xi}$$

Numerical Methods. The nine Zeeman product functions of the two-spin system were chosen as base functions for the matrix representation of the Hamiltonians. From these, the 81 Liouville space base functions of the Liouville space were constructed and the Liouville, exchange, and relaxation operators were expressed in these base functions and combined to the dynamic superoperator \hat{M} . To reduce the computational problem, these base functions were arranged according to their multiple quantum order, which transforms \hat{M} into a block diagonal form. In the calculations we started with the initial condition that a 90° pulse was applied to the spin system in thermal equilibrium, and thus the initial density matrix $|\rho(0)\rangle$ is given by $|F_x\rangle$:

$$|\rho(0)\rangle = |F_x\rangle = |I_{x1} + I_{x2}\rangle \quad (36)$$

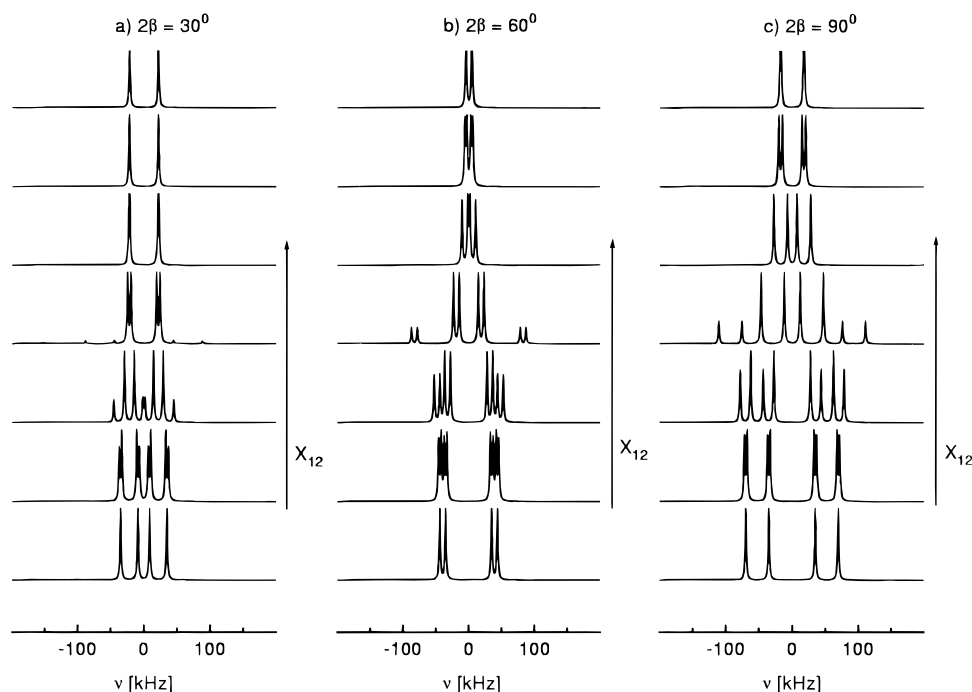


Figure 3. Simulation of coherent exchange (tunneling) in the ^2H NMR spectra of a single crystal for three different relative orientations of the two quadrupole tensors. The external magnetic field is parallel to the principal axis corresponding to q_{zz} of the first tensor. $q_{zz} = 70$ kHz, $\eta = 0$, $X_{12} = 0, 2, 32, 128, 512, 2048, 8192$ kHz. In contrast to the incoherent exchange, the spectra exhibit splittings instead of broadening. The spectrum for $X_{12} \gg \Delta q$ is identical to the fast incoherent exchange spectrum.

The density operator of the system and the \hat{M} superoperator were expressed in the base of the Liouville space described above. The resulting spectra were calculated by diagonalization of \hat{M} using a routine from LAPACK¹⁹ and transforming the detection operator and the density operator into the eigenbase of \hat{M} . The powder averages were calculated by integrating over a grid of 128×128 equally spaced polar angles φ and ϑ .

Results and Discussion

In the following, we want to present the results of our calculations. For both deuterons, an axial symmetric quadrupole tensor ($\eta = 0$) with $q_{zz} = 70$ kHz was used, which we have estimated from the room temperature spectra of the Ru-D₂ complexes currently under experimental observation (see Discussion). The spectra were calculated for different relative orientations β of the two tensors, varying from $2\beta = 0^\circ$ to $2\beta = 90^\circ$. Since for $2\beta = 0^\circ$ the quadrupole tensors of the two deuterons are collinear, the spectra are influenced by neither coherent nor incoherent exchange. Before some typical numerical results are shown, some general properties of the results will be discussed. First it should be noted that the principal difference between a coherent and an incoherent exchange is that the coherent exchange will, in general, lead to a shift of the energy levels and thus to a splitting of the transition frequencies, while the incoherent exchange will cause a line broadening or line coalescence of the transition frequencies. While these effects will be most pronounced in single-crystal spectra, where only few transition frequencies are present, taking the powder average will inevitably cause a blurring of these differences. Thus, for discussing the principal differences of coherent versus incoherent exchange, it is most suitable to calculate single-crystal spectra, while for real life samples, one has to calculate the powder spectrum. The question is whether these spectra will show enough characteristic features to distinguish between coherent and incoherent exchanges.

Results for Single Crystals. For purely incoherent exchange, the spectra exhibit the typical incoherent exchange scenario:^{12b} line broadening of the NMR lines for small exchange rates; line coalescence at exchange rates on the order of the difference of the quadrupole splitting; again line narrowing at fast exchange rates; full motional averaging of the difference of the quadrupole splitting in the spectrum at very fast exchange rates.

Figure 3 shows the effects of purely coherent tunneling on the spectra for three different relative orientations of the quadrupole tensors. The external magnetic field is chosen parallel to the principal axis corresponding to the z -component of the quadrupole tensor of deuteron 1. While the spectra for $2\beta = 0^\circ$ are not affected by the exchange, for the other angles the spectra exhibit a distinctively different behavior. For small coherent exchange frequencies, a splitting of the lines into doublets is observed. This splitting increases with the coherent exchange frequency. For coherent exchange frequencies on the order of the quadrupole splitting, the intensity ratio of the lines changes and typical higher order NMR spectra are observed, where the main line intensities are at the inner transitions. Moreover, the splitting of the inner pair of lines narrows, while the splitting of the outer lines increases with the coherent exchange frequency. However, for coherent exchange frequencies much larger than the difference of the quadrupole coupling constants, once more a simple two-line spectrum is observed, which is identical with the corresponding spectrum for incoherent exchange. The differences between coherent exchange and incoherent exchange are most pronounced for rates on the order of the quadrupole splitting. The incoherent exchange broadens the lines so strongly that their relative amplitude compared to the amplitude of the spectra for low or high rates is close to zero in the coalescence regime. The coherent tunneling, however, leads to splittings of the lines into doublets, and in particular the relative amplitude of the central lines is only weakly affected by the tunneling.

Figure 4 displays the effect of the simultaneous presence of coherent and incoherent exchange. The spectra show the effect

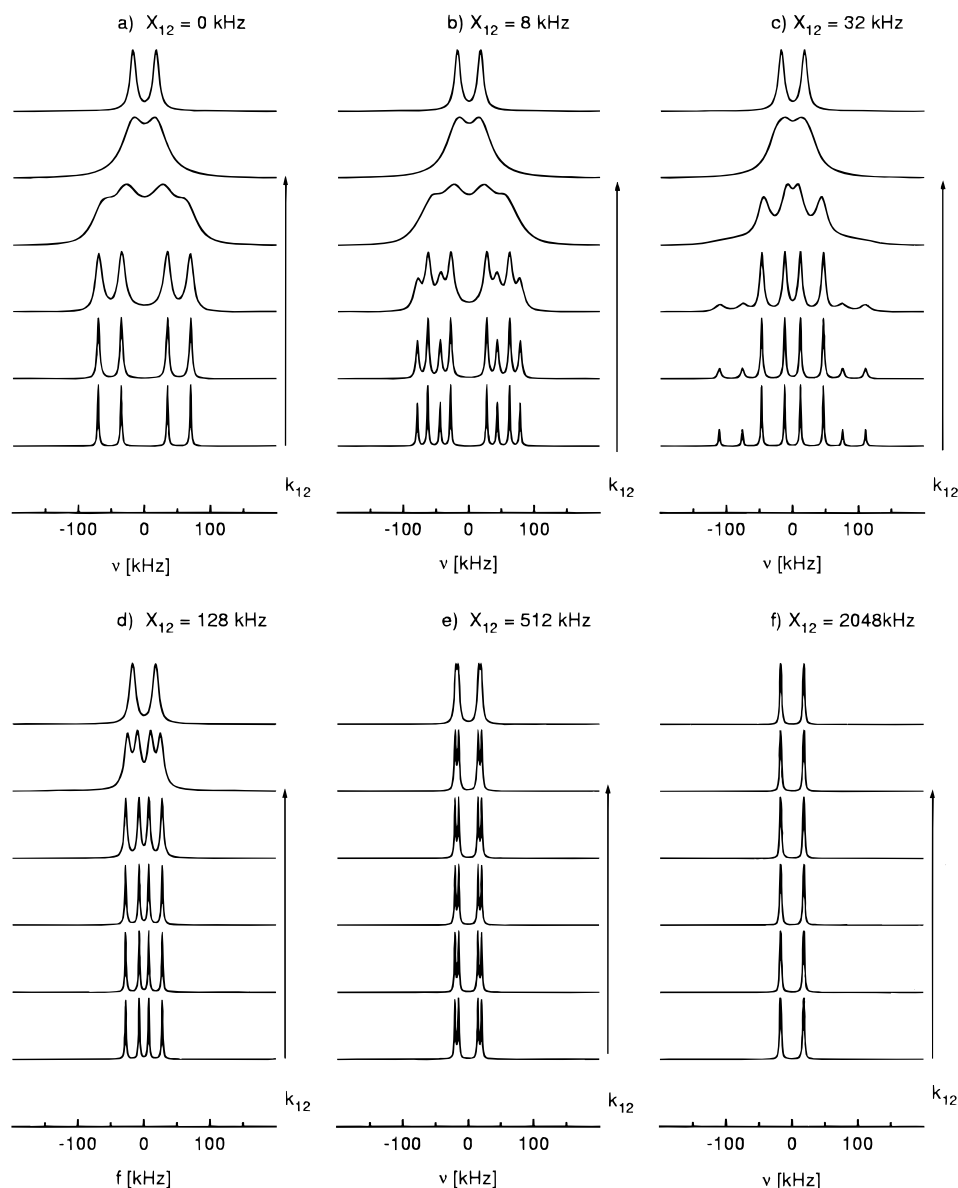


Figure 4. Simulation of simultaneous incoherent and coherent exchange (tunneling). $q_{zz} = 70$ kHz, $\eta = 0$, $k_{12} = 0, 8, 32, 128, 512, 2048$ kHz. The external magnetic field is parallel to the principal axis corresponding to q_{zz} of the first tensor. The second tensor is rotated with $2\beta = 90^\circ$ with respect to the first tensor. The relative size of coherent and incoherent exchange rates determine the shape of the spectral lines.

of incoherent exchange for different coherent exchange frequencies. While for the lowest coherent exchange frequency the effect of incoherent exchange is immediately visible in the spectra, for increasing coherent exchange frequency the incoherent exchange rate has to be increased to have a visible effect on the spectra. In particular the broadening of the lines starts for incoherent exchange rates on the order of the coherent exchange frequency, while for incoherent exchange rates far below the coherent frequency, the effects of the incoherent exchange are not visible. In other words, the shape of the spectra is determined by the relative speed of coherent versus incoherent exchange. Moreover this faster rate must be at least on the order of the difference of the quadrupole splitting to have an effect on the spectra.

Results for Powder Samples. The upper part of Figure 5 depicts the effects of incoherent exchange of the two deuterons as a function of the rotation angle 2β for randomly oriented powder samples, which are the typical incoherent exchange spectra known from NMR experiments on various deuterated systems.^{17c} As in the case of single crystals, the effect of the incoherent exchange is most pronounced for $2\beta = 90^\circ$, while the $2\beta = 0^\circ$ spectra (not shown) are not affected by the exchange of the deuterons. The exchange first causes a smearing of the

edges of the Pake pattern and then the typical formation of a narrowed Pake pattern, whose asymmetry parameter depends on the angle between the two tensors. The lower part of Figure 5 displays the results of the same calculations for the case of coherent exchange of the two different deuterons. While for small or large coherent exchange frequency these spectra are practically indistinguishable from the spectra of incoherent exchange, there are pronounced differences for intermediate spectra, where the coherent exchange frequency is on the order of the quadrupole coupling. For these spectra, the satellite transitions, which have appeared in the single-crystal spectra, lead to spectral contributions outside the range of the spectra without coherent exchange. Moreover in this intermediate range, the singularities in the spectra appear much sharper than the singularities in the corresponding incoherent exchange spectra.

Figure 6 finally shows the calculation of powder spectra, where both coherent and incoherent exchange are simultaneously present. As has already appeared in the corresponding calculations of single-crystal spectra, for this type of combined exchange the relative sizes of coherent tunnel versus incoherent exchange rate determine the shape of the NMR spectra. If the coherent exchange frequency is small (Figure 6a), i.e. $X_{12} \ll$

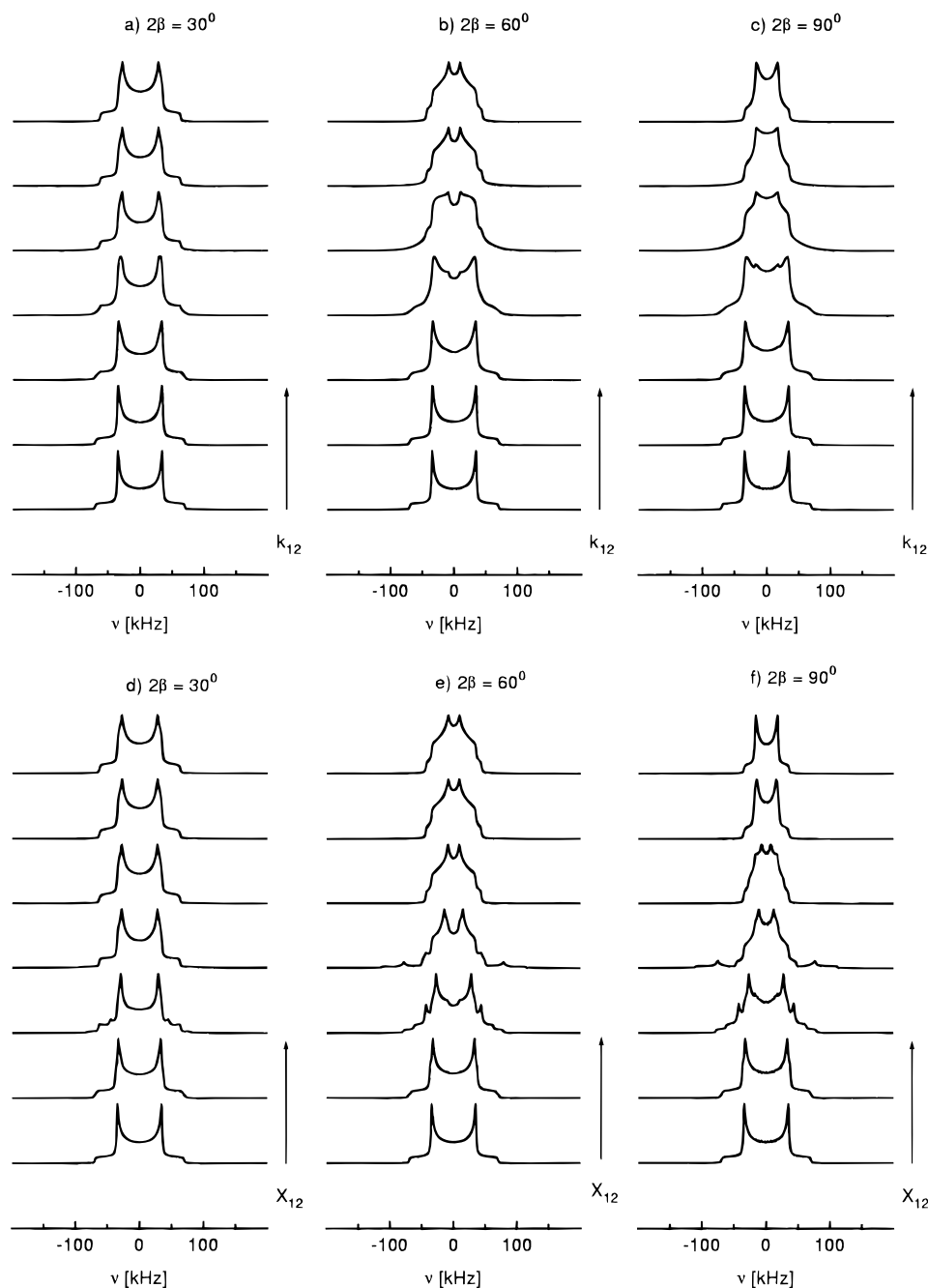


Figure 5. Effects of coherent and incoherent exchange on the ^2H NMR spectra of a nonoriented powder sample (powder spectra) for the same three relative orientations of the quadrupole tensors as in Figure 3. Upper row: simulation of incoherent exchange. $q_{zz} = 70$ kHz, $\eta = 0$, $k_{12} = 0, 2, 32, 128, 512, 2048, 8192$ kHz. The exchange mainly leads to a smearing of the edges of the Pake pattern, which for higher rates narrows to the average spectrum. Lower row: simulation of coherent exchange: $q_{zz} = 70$ kHz, $\eta = 0$, $X_{12} = 0, 2, 32, 128, 512, 2048, 8192$ kHz. In the intermediate range of coherent exchange frequencies, there are satellite lines, which clearly distinguish the spectra from the corresponding incoherent spectra.

Q , the spectra exhibit exactly the same behavior as the spectra without coherent exchange (Figure 5c). On the other hand, for a fast coherent exchange ($X_{12} \gg Q$), the spectra do not depend on the incoherent exchange (Figure 6f). In the intermediate regime, $X_{12} \approx Q$, the spectra exhibit a rather complicated line shape, which nevertheless still shows the sharp features of the coherent tunneling line shape. Again, for all coherent exchange frequencies, the spectra at fast incoherent rates are identical, and only for intermediate exchange rates an effect on the spectra is visible.

Discussion. To summarize the results of the numerical calculations: It has been shown that there are pronounced differences between coherent and incoherent exchange of two deuterons in the ^2H NMR spectra of these deuterons. In particular, the former leads to a splitting of the spectral lines, while the latter leads first to a broadening and later to a

narrowing of the lines, which can be interpreted as a relaxation of coherences between states of different symmetry with respect to particle permutation. It has been found that these differences are most pronounced for coherent exchange frequencies which are on the order of the quadrupole coupling constant. Thus by investigation of this range of intermediate tunnel splitting, we expect that it is possible not only to distinguish between coherent and incoherent exchange but also to determine the size of the tunnel splitting. The actual effect on the spectra depends strongly on the configuration of the quadrupole tensors associated with the two deuterons. If these tensors are collinear, the spectra are affected neither by coherent nor by incoherent exchange. If, on the other hand, the two tensors are rotated 90° relative to each other, the effect is most pronounced. The simulations show that the effects are best visible in single

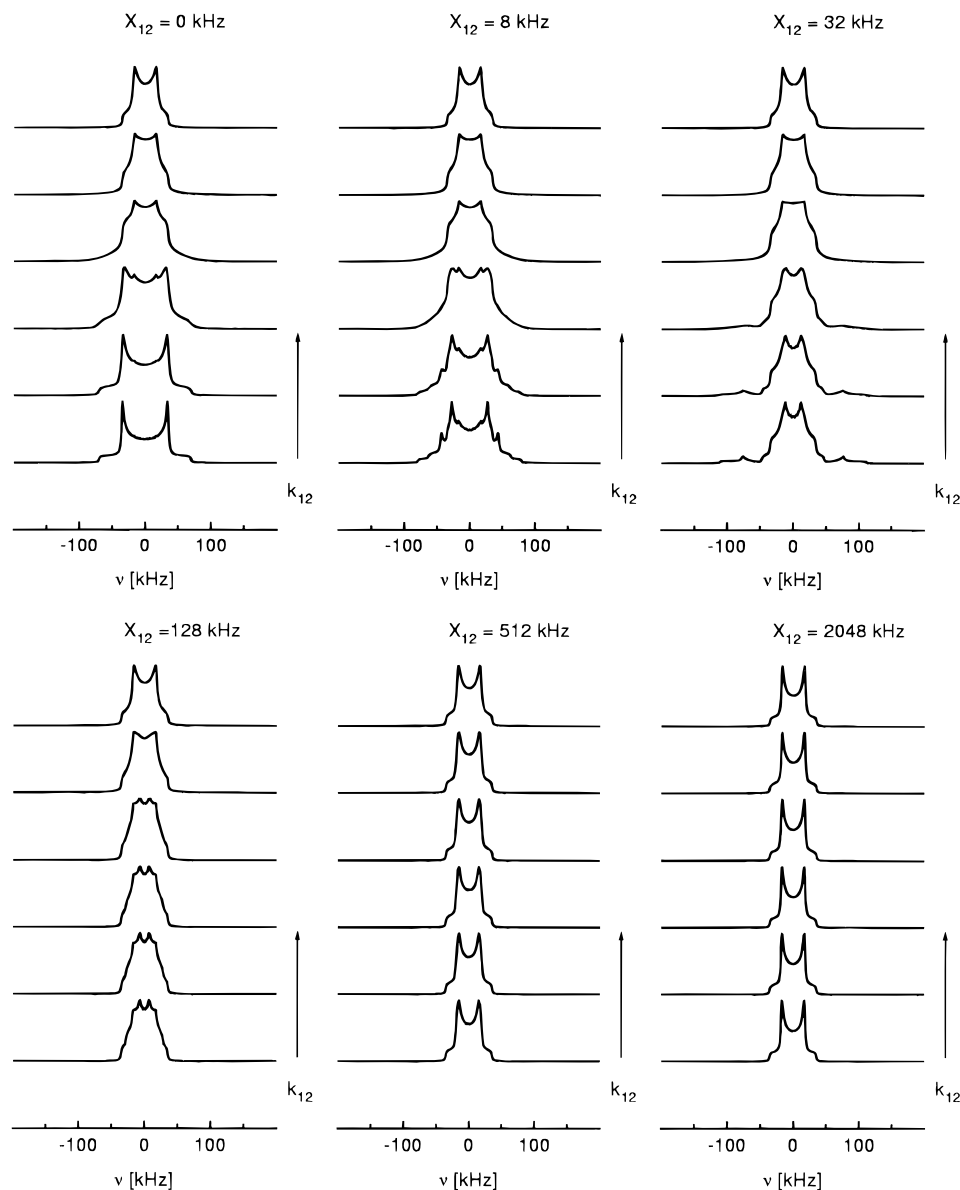


Figure 6. Simulation of simultaneous incoherent and coherent exchange (tunneling) for the same relative orientations and parameters: $2\beta = 90^\circ$, $q_{zz} = 70$ kHz, $\eta = 0$, $X_{12} = 0, 8, 32, 128, 512, 2048$ kHz as in Figure 5. The relative size of coherent and incoherent exchange rates determine the shape of the spectral lines. Note in particular that for X_{12} or $k_{12} \gg \Delta q$, the shape of the spectra does not depend on the second kind of exchange process.

crystals. However, also for powdered samples the differences should be clearly visible in experimental spectra.

The remaining question is thus whether it is feasible to detect these processes in actual experiments. In such experiments several difficulties must be overcome. On the one hand, the coherent exchange frequency, which depends very strongly on the depth of the hindering potential for the rotation, must fall into the "proper" range of frequencies, as discussed above. As simple estimations with a one-dimensional hindered rotor show, employing a 2-fold potential with a cosine type of angular dependence, only for a very small range of the potential depth, the coherent exchange frequency is in the NMR frequency regime. In particular, changing the potential depth by a factor of 10 in this NMR sensitive regime leads to a change of the coherent tunnel frequency by a factor of 10^{11} . We expect this strong dependence to be at least partially weakened by the fact that for the considered transition metal dihydrides, the radial potential varies weaker with the radius, as compared for example to covalently bound deuterons in tunneling methyl groups, leading to a weaker dependence of the tunnel splitting on the potential depth or the deuteron distance. However, because of

the small accessible frequency window, choosing the right substance is no trivial task.

The biggest experimental difficulty, however, stems from sensitivity problems caused by low deuterium abundance. We have performed preliminary ^2H -NMR experiments on a selectively deuterated transition metal dihydride (molecular formula: $\text{C}_{52}\text{H}_{48}\text{ClD}_2\text{F}_6\text{P}_5\text{Ru}$, MW = 1082 g/mol), which, to the best of our knowledge, is the first selectively deuterated solid transition metal dihydride. Due to its high molecular weight, the amount of deuterium in the sample is rather low, resulting in a poor NMR sensitivity of the sample, as compared for example to organic compounds where tunneling in deuterated methyl groups¹⁴ (e.g. aspirin- CD_3) has been studied. There, the amount of deuterium in the sample can be estimated to be about 5–10 times higher than in the transition metal dihydride. The room-temperature ^2H -NMR spectra of the transition metal dihydride compound exhibited a motionally averaged line with a width of about 50 kHz and T_1 relaxation times of several seconds, which are comparable to methyl groups. Thus the amount of deuterium can be used to quantitatively compare the sensitivity of our transition metal dihydride sample to the

deuterated methyl groups, resulting in approximately 5–10 times lower sensitivity. From this lower sensitivity it follows that artifacts, caused for example by dead time problems or acoustic ringing, will have a much stronger effect on the low-temperature $^2\text{H-NMR}$ spectra of our compound, as compared to the deuterated methyl groups. However, this should not make the experiments unfeasible. Thus we finally wish to conclude that the proposed usage of a deuterated transition metal dihydride for the study of coherent tunnel frequencies in the regime of 10^5 Hz is feasible.

Acknowledgment. The authors express their special gratitude to Herrn Andreas Detken, MPI für Medizinische Forschung, Heidelberg, for his careful reading and critical discussion of the manuscript and the underlying physics. This work was supported by the Deutsche Forschungsgemeinschaft, Bonn-Bad Godesberg, and the Fonds der Chemischen Industrie, Frankfurt.

References and Notes

- (1) (a) Kubas, G. J.; Ryan, R. R.; Swanson, B. I.; Vergamini, P. J.; Wasserman, H. J. *J. Am. Chem. Soc.* **1984**, *116*, 451. (b) Kubas, G. J. *Acc. Chem. Res.* **1988**, *21*, 120.
- (2) (a) Rattan, G.; Kubas, G. J.; Unkefer, C. J.; Van Der Sluys, L. S.; Kubat-Martin, K. A. *J. Am. Chem. Soc.* **1990**, *112*, 3855. (b) Eckert, J.; Kubas, G. J. *J. Phys. Chem.* **1993**, *97*, 2378. (c) Eckert, J.; Jensen, C. M.; Jones, G.; Clot, E.; Eisenstein, O. *J. Am. Chem. Soc.* **1993**, *115*, 11056.
- (3) Jessop, P. G.; Morris, R. J. *Coord. Chem. Rev.* **1992**, *121*, 155.
- (4) (a) Arliguie, T.; Chaudret, B.; Devillers, J.; Poilblanc, R. *C. R. Acad. Sci. Paris, Ser. II*, **1987**, *305*, 1523. (b) Antinolo, A.; Chaudret, B.; Commenges, G.; Fajardo, M.; Jalon, F.; Morris, R. H.; Otero, A.; Schweitzer, C. T. *J. Chem. Soc., Chem. Commun.* **1988**, 1210. (c) Arliguie, T.; Border, C.; Chaudret, B.; Devillers, J.; Poilblanc, R. *Organometallics* **1989**, *8*, 1308. (d) Arliguie, T.; Chaudret, B.; Jalon, F. A.; Otero, A.; Lopez, J. A.; Lahoz, F. J. *Organometallics* **1991**, *10*, 1888. (e) Paciello, R. R.; Manriquez, J. M.; Bercaw, J. E.; *Organometallics* **1990**, *9*, 260. (f) Heinekey, D. M.; Payne, N. G.; Schulte, G. K. *J. Am. Chem. Soc.* **1988**, *110*, 2303. (g) Heinekey, D. M.; Millar, J. M.; Koetzle, T. F.; Payne, N. G.; Zilm, K. W. *J. Am. Chem. Soc.* **1990**, *112*, 909. (h) Limbach, H. H.; Scherer, G.; Meschede, L.; Aguilar-Parrilla, F.; Wehrle, B.; Braun, J.; Hoelger, Ch.; Benedict, H.; Buntkowsky, G.; Fehlhammer, W. P.; Elguero, J.; Smith, J. A. S.; Chaudret, B. NMR Studies of Elementary Steps of Hydrogen Transfer in Condensed Phases. In *Ultrafast Reaction Dynamics and Solvent Effects, Experimental and Theoretical Aspects*; Gauduel, Y., Rossky, P. J., Eds.; American Institute of Physics: New York 1994; Chapter 2, p 225. (i) Antinolo, A.; Carrillo, F.; Chaudret, B.; Fajardo, M.; Fernandez-Baeza, J.; Lanfranchi, M.; Limbach, H. H.; Maurer, M.; Otero, A.; Pellinghelli M. A. *Inorg. Chem.* **1994**, *33*, 5163. (k) Ayllon, J. A.; Sabo-Etienne, S.; Chaudret, B.; Ulrich, S.; Limbach, H. H. *Inorg. Chem.*, in press.
- (5) (a) Zilm, K. W.; Heinekey, D. M.; Millar, J. M.; Payne, N. G.; Demou, P. *J. Am. Chem. Soc.* **1989**, *111*, 3088. (b) Zilm, K. W.; Heinekey, D. M.; Millar, J. M.; Payne, N. G.; Neshyba, S. P.; Duchamp, J. C.; Szczyrba, J. *J. Am. Chem. Soc.* **1990**, *112*, 920. (c) Zilm, K. W.; Millar, J. M. *Adv. Magn. Reson.* **1990**, *15*, 16. (d) Inati, S. J.; Zilm, K. W. *Phys. Rev. Lett.* **1992**, *68*, 3273. (e) Jones, D.; Labinger, J. A.; Weitekamp, J. J. *J. Am. Chem. Soc.* **1989**, *111*, 3087. (f) Szymanski, S. *J. Mol. Struct.* **1994**, *321*, 115.
- (6) Limbach, H. H.; Scherer, G.; Maurer, M.; Chaudret, B. *Angew. Chem.* **1992**, *104*, 1414; *Angew. Chem., Int. Ed. Engl.* **1990**, *31*, 1369.
- (7) (a) Barthelat, J. C.; Chaudret, B.; Dauday, J. P.; De Loth, Ph.; Poilblanc, R. *J. Am. Chem. Soc.* **1991**, *113*, 9896. (b) Jarid, A.; Moreno, M.; Lledós, A.; Lluch, J. M.; Bertran, J. *J. Am. Chem. Soc.* **1993**, *115*, 5861. (c) Jarid, A.; Moreno, M.; Lledós, A.; Lluch, J. M.; Bertran, J. *J. Am. Chem. Soc.* **1995**, *117*, 1069. (d) Clot, E.; Leforestier, C.; Eisenstein, O.; Pelissier, M. *J. Am. Chem. Soc.* **1995**, *117*, 1797.
- (8) Buntkowsky, G.; Bargon, J.; Limbach, H. H. *J. Am. Chem. Soc.* **1996**, *30*, 8677.
- (9) Alexander, S. *J. Chem. Phys.* **1962**, *37*, 971.
- (10) (a) Binsch, G. *J. Am. Chem. Soc.* **1969**, *91*, 1304. (b) Kleier, D. A.; Binsch, G. *J. Magn. Reson.* **1970**, *3*, 146.
- (11) Szymanski, S. *J. Chem. Phys.* **1996**, *104*, 8216.
- (12) (a) Abragam, A. *Principles of Nuclear Magnetism*; Clarendon Press: Oxford, 1961; Chapter VII. (b) Slichter, C. P. *Principles of Magnetic Resonance*, 3rd ed.; Springer: Berlin, Heidelberg, New York, 1990. (c) Schmidt-Rohr, K.; Spiess, H. W. *Multidimensional Solid-State NMR and Polymers*; Academic Press: London, 1994.
- (13) Pake, G. E. *J. Chem. Phys.* **1948**, *16*, 327.
- (14) (a) Bernhard, T.; Haeberlen, U. *Chem. Phys. Lett.* **1991**, *186*, 307. (b) Detken, A.; Focke, P.; Zimmermann, H.; Haeberlen, U.; Olejniczak, Z.; Lalowicz, Z. T. *Z. Naturforsch.* **1995**, *50a*, 95. (c) Lalowicz, Z. T.; Werner, U.; Müller-Warmuth, W. *Z. Naturforsch.* **1988**, *43a*, 219. (d) Szymanski, Olejniczak, H.; Haeberlen, U. *Physica B* **1996**, **226**, 161.
- (15) Dirac, P. A. M. *Quantum Mechanics*, 4th ed.; Oxford University Press: London, 1958.
- (16) (a) Schlabach, M.; Rumpel, H.; Limbach, H. H. *Angew. Chem.* **1989**, *101*, 84; *Angew. Chem., Int. Ed. Engl.* **1989**, *28*, 78. (b) Schlabach, M.; Scherer, G.; Limbach, H. H.; *J. Am. Chem. Soc.* **1991**, *113*, 3550. (c) Braun, J.; Limbach, H. H.; Williams, P.; Morimoto, H.; Wemmer, D. *J. Am. Chem. Soc.* **1996**, *30*, 7231. (d) Scheurer, Ch.; Widenbruch, R.; Meyer, R.; Ernst, R. R. Submitted for publication in *J. Chem. Phys.*
- (17) Messiah, A. *Quantum Mechanics*; North Holland Publishing Company: Amsterdam, 1970; Vol. II.
- (18) Ernst, R. R.; Bodenhausen, G.; Wokaun, A. *Principles of NMR in One and Two Dimensions*; Clarendon Press: Oxford, 1987.
- (19) LAPACK Program package, University of California, Berkeley, 1994; email address: netlib@research.att.com.